Studying the effect of expanding low or high frequency on post-stack seismic inversion

Xi Xiaoyu, Ling Yun, Sun Desheng, Guo Xiangyu, Wang Huifeng, BGP, CNPC*

Summary

It is generally difficult to expand high-frequency effective reflection information of seismic migration because of factors such as earth attenuation, high-frequency noise, etc. Due to this, scholars focus on whether low-frequency effective reflection information can be expanded. Some research has found it useful to directly obtain seismic velocity of propagation by expanding middle and low-frequency effective reflection information of seismic migration. However, it is important to understand the effect of expanding high or low-frequency effective reflection information on seismic inversion, and to determine whether the higher resolution data or more accurate seismic velocity can be obtained. To address these issues, based on 3D thin-bed geologic model and post-stack linear programming inversion method (LP), we study the influence of expanding high or low-frequency effective reflection information on seismic inversion by the inversion of synthetic seismic data with different high frequencies missing and different low frequencies missing. Our study indicates that the recognition capability of thin-bed reservoirs cannot be improved by adding low-frequency information of seismic migration data, although the frequency band of seismic data can be expanded, and the apparent resolution of seismic data and accuracy of obtaining seismic impedance can be improved. We also find that the recognition capability of impedance interface and impedance accurateness can be improved by adding high-frequency information of seismic migration data.

Introduction

Seismic impedance inversion, under the assumption of plane-wave propagation, time-invariant seismic signal, and multiple and ghost free reflection, stems from the synthesis of seismograms from well log data presented by Peterson et al. (1955) and Sengbush et al. (1961). Following them, Lindseth (1979) and Becquey et al. (1979) developed Seislog inversion theory, which enabled people to recognize and interpret some geologic phenomena from impedance data. Then, many scholars made further mathematical studies, formulating diverse approaches of inversion such as Sparse Spike Inversion (Levy and Fullagar, 1981), Recursion Inversion on the basis of discrete model and continuous model (Berteussen and Ursinl, 1983), Autoregression Inversion (Walker and Ulrych, 1983), Generalized Linear Inversion (Cooke and Schneider, 1983) or L2 inversion, Global Stochastic Seismic Inversion (Maver et al., 1994) and Seismic Feature Inversion (Debeye, 1995), and so on. With the development of various post-stack impedance inversion methods, it has been gradually recognized that many factors contribute to the applicability for the different approaches. Francis (1997) discussed the pitfalls of inversion from seismic data processing pre-inversion (such as synthetic seismograms from well log data, well-seismic data calibration, and low frequency model etc.) to impedance interpretation post-inversion. Huang et al. (1995) studied the effect of wavelet on inversion, including its frequency, phase and time, and found that wavelet bandwidth influenced inversion remarkably, while its phase and duration displayed little influence.

However, the above studies assume that seismic data are band-limited. Namely, that seismic data are short of high frequency and low frequency. This phenomenon is caused by seismic acquisition, earth attenuation, high-frequency noise, etc., and it has a bad influence on geologic interpretations of seismic data. This paper mainly focuses on the effect of expanding low or high frequency on seismic post-stack inversion, which is helpful to understand whether it is necessary to obtain the broad-band seismic data via novel equipment in seismic acquisition or special seismic processing techniques.

Geologic model and synthetic seismic data

The geologic model used for the seismic inversion consists of two thin sand bodies with irregular borders and variable thickness in space, and a channel with differing widths and spatial-variant thicknesses. Time slice of velocity, velocity curves of the three analyzed points and section of velocity along the diagonal line are shown in Figure 1a, 1b and 1c. Figure 1d is the reflection coefficient section of the geologic model along the diagonal line. Figure 1a also shows the position of three analyzed points: point 1 is located in one thin sand body, point 2 is on the channel, and point 3 is situated in the locations outside of the sand bodies and the channel. From Figure 1b, we can see theoretical velocity curves of the three analyzed points. The density of the model is constant (equal to 1), so the impedance are the same as the velocity in numerical value. In Figure 1c, velocity changes continuously in the vertical direction, and velocity changes abruptly on the thin sand, channel and impedance interface.

Based on above geologic model, synthetic seismic data are obtained by the convolution theory. These seismic data meet the ideal requirement for seismic inversion, such as plane wave, time-invariant seismic signal, and multiple and ghost free reflection. Figure 2 presents synthetic sections by convolution of 0-0-100-300Hz wavelet with low frequency and wide frequency band (Figure 2a), 0-0-60-120Hz wavelet with low frequency and observed seismic frequency band (Figure 2b), 5-10-60-120Hz wavelet with no low frequency and observed seismic frequency band (Figure 2c) and

DOI http://dx.doi.org/10.1190/segam2012-0146.1

10-20-60-120Hz wavelet with no more low frequency and observed seismic frequency band (Figure 2d) respectively. From Figure 2, we can see that forward-modeling seismic data contain seismic data without different high frequencies and low frequencies. The influence of expanding low or high frequencies will be analyzed by using these forward-modeling seismic data in seismic post-stack inversion.

The influence of expanding low or high frequencies

The linear programming method for post-stack seismic inversion without a frequency band constraint is chosen in this study. The reason for this is that with this method, the inversion result has a broad frequency band when seismic data do not contain noise, especially high-frequency noise. Due to this, we can effectively analyze the effect of expanding high/low frequency on seismic inversion.

Figure 3 shows the corresponding inversion result of synthetic seismic data. From Figure 3, we can see that:

(1) In Figure 3a, the inversion result of seismic data with low frequency and wide frequency band (0-0-100-300Hz) is similar to the geologic model.

(2) In Figure 3b, there are some errors at the impedance interface and pinchout boundary of sand in the inversion result with low frequency and without part of the high frequency (0-0-60-120Hz), when compared with Figure 3a.

(3) Figure 3c and 3d are the inversion results without low frequency and part of high frequency (5-10-60-120Hz and 10-20-60-120Hz). Comparing these results with Figure 3b, our results show that spatial instability and errors increase with more low-frequencies missing, except that errors exist at impedance interface. The recognition capability of thin-bed reservoirs, the thin sands and channel, is almost the same.

Figure 4 shows the inversed impedance curves and error between the true impedance and inversed impedance at the three analyzed points. Figure 4a is the true impedance curves. Figure 4b, 4c, and 4d are the corresponding inversed impedance curves and error between inversed and the true impedance. From Figure 4, we can see that:

(1) For inversed curves of seismic data with low frequency and wide frequency band (0-0-100-300Hz), there is a small error between the inversed (pink) and true (red) impedance, and the error exists mainly at the part of impedance mutation. This means that with the increase of high frequency of seismic migration data, the inversion result is close to the true impedance. The lack of high frequency in seismic migration data mainly has an influence on the resolution and accuracy of seismic inversion result.

(2) For inversed curves of seismic data with low frequency and without part of the high frequency (0-0-60-120Hz), there is large error between inversed (blue) and the true (red) impedance, and the error exists mainly at the part of impedance mutation. Comparing this with Figure 4a, the error becomes larger. This demonstrates further that the lack of high frequency seismic migration data mainly has an influence on the resolution and accuracy of the seismic inversion result.

(3) For inversion curves of seismic data without low frequency and part of high frequency (5-10-60-120Hz and 10-20-60-120Hz), there is large error between the inversed (light blue and black) and true (red) impedance, and the error mainly exists at the part of continuous impedance change, not at the part of impedance mutation. This suggests that the lack of low frequency has an influence on the vertical trend and accuracy of the inversion result.

Conclusions

From above analysis, some conclusions can be reached that the lack of high frequency in seismic migration data causes error mainly at the part of impedance mutation. The lack of low frequency causes error of the vertical impedance trend. In seismic inversion, adding low frequency in seismic acquisition and processing can improve the accuracy and capability of seismic inversion. However, adding low frequency cannot improve the resolution of seismic inversion. If we want to improve the resolution of seismic inversion, high frequency must be added in the acquisition and processing of seismic data.

DOI http://dx.doi.org/10.1190/segam2012-0146.1

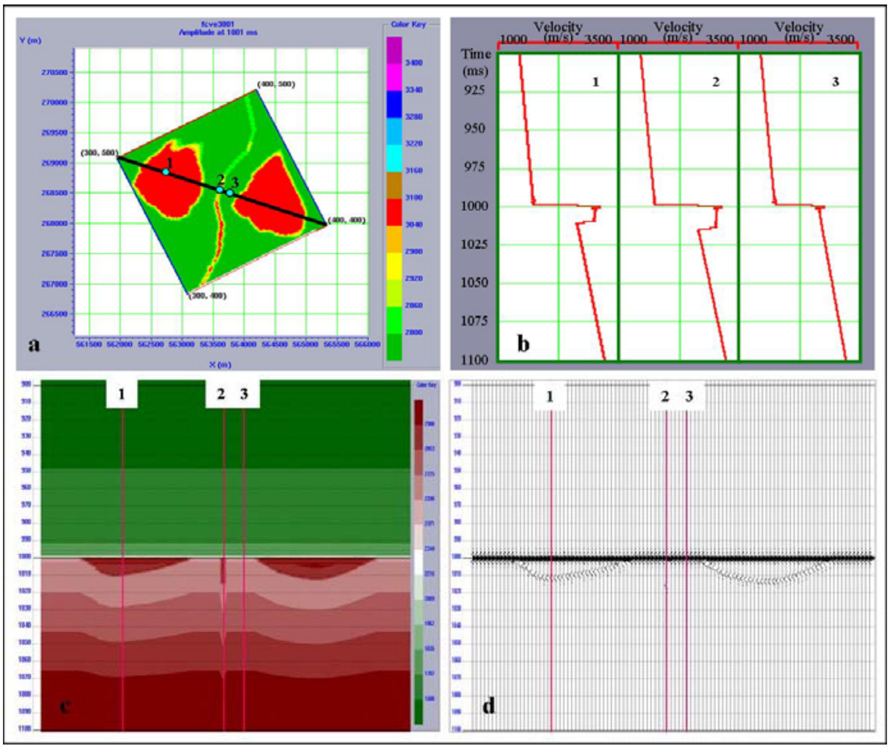

Figure 1: The geologic model: a) velocity slice; b) velocity curves of corresponding analyzed points in figure 1a; c) velocity section along the diagonal line; d) reflection coefficient section along the diagonal line.

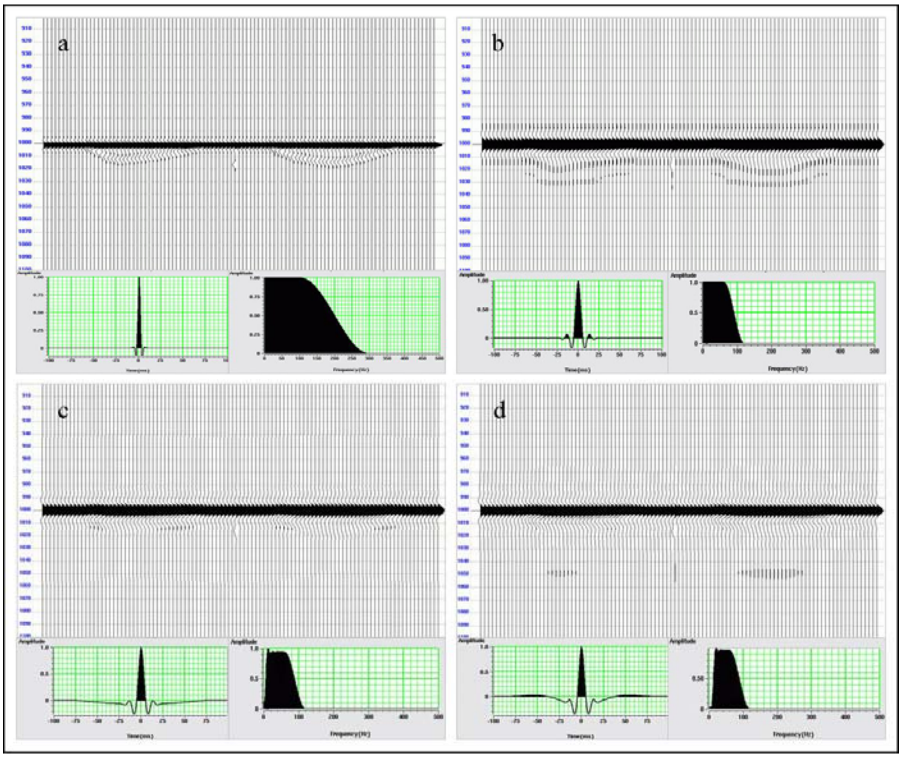

Figure 2: Synthetic sections by convolution of 0-0-100-300Hz wavelet (a), 0-0-60-120Hz wavelet (b), 5-10-60-120Hz wavelet (c), and 10-20-60-120Hz wavelet (d). The corresponding wavelets are below synthetic sections.

DOI http://dx.doi.org/10.1190/segam2012-0146.1

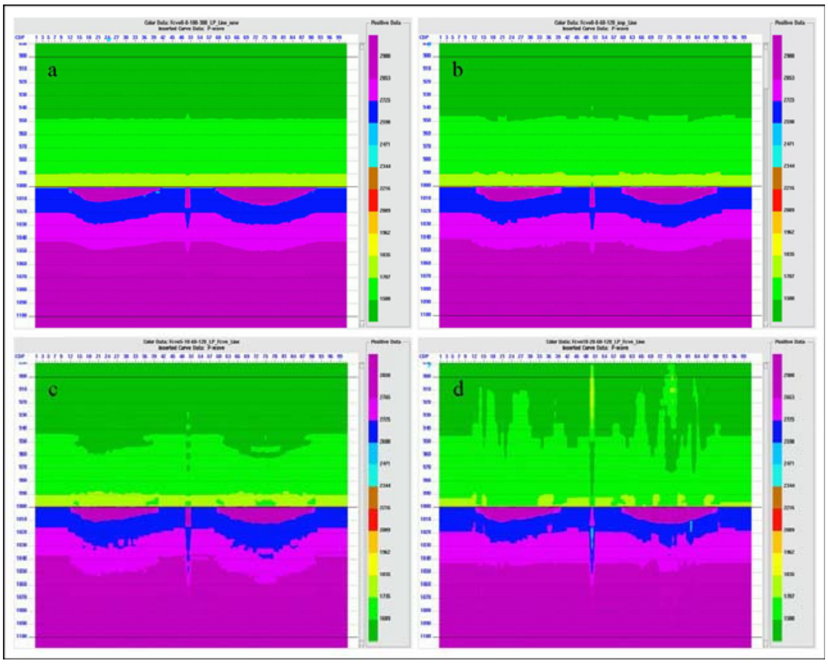

Figure 3: Inversion sections of synthetic seismic data by convolution of 0-0-100-300Hz wavelet (a), 0-0-60-120Hz wavelet (b), 5-10-60-120Hz wavelet (c), and 10-20-60-120Hz wavelet (d).

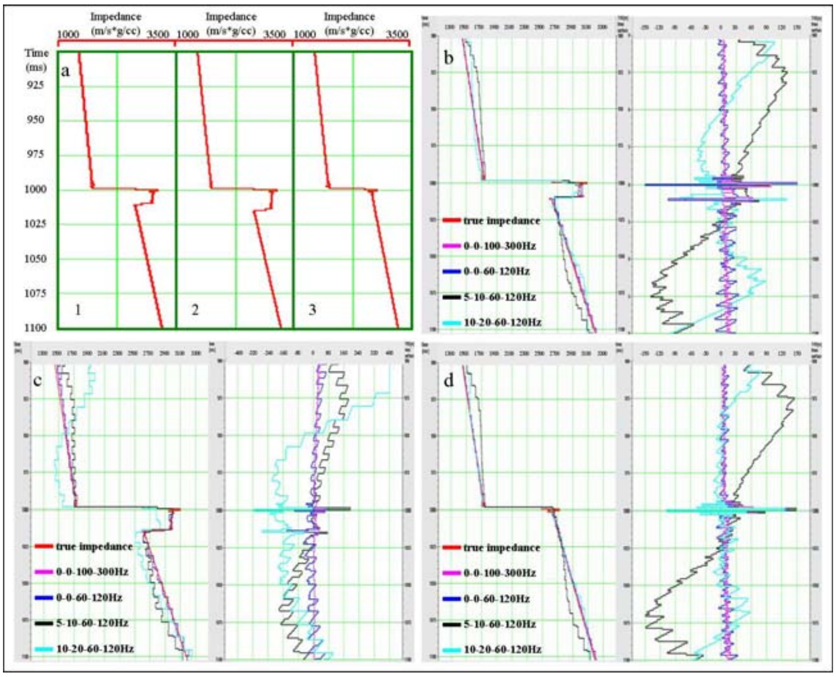

Figure 4: Impedance curves and the mismatch between the true impedance and inversed impedance: a) true impedance of the three analyzed points. b) Impedance curves and error at point 1. c) Impedance curves and error at point 2. d) Impedance curves and error at point 3. For Figure 4b, 4c and 4d, red lines stand for true impedance in the left panel. Pink lines are inversed impedance of synthetic seismic data of 0-0-100-300Hz wavelet in the left figure or impedance error in the right figure between true impedance and inversed impedance of 0-0-100-300Hz seismic data. Blue lines are inversed impedance of synthetic seismic data of 0-0-60-120Hz wavelet in the left figure or impedance error in the right figure between true impedance and inversed impedance of 0-0-60-120Hz seismic data. Black lines are inversed impedance of synthetic seismic data of 5-10-60-120Hz wavelet in the left figure or impedance error in the right figure between true impedance and inversed impedance of 5-10-60-120Hz seismic data. Light blue lines are inversed impedance of synthetic seismic data of 10-20-60-120Hz wavelet in the left figure or impedance error in the right figure between the true impedance and inversed impedance of 10-20-60-120Hz seismic data.

DOI http://dx.doi.org/10.1190/segam2012-0146.1

http://dx.doi.org/10.1190/segam2012-0146.1

EDITED REFERENCES

Note: This reference list is a copy-edited version of the reference list submitted by the author. Reference lists for the 2012 SEG Technical Program Expanded Abstracts have been copy edited so that references provided with the online metadata for each paper will achieve a high degree of linking to cited sources that appear on the Web.

REFERENCES

Becquey M., M. Lavergne, and C. Willm, 1979, Acoustic impedance logs computed from seismic traces: Geophysics, **44**, 1485–1501.

Berteussen K. A., B. Ursinl, 1983, Approximate computation of the acoustic impedance from seismic data: Geophysics, **48**, 1351–1358.

Cooke D. A., and W. A. Schneider, 1983, Generalized inversion of reflection seismic data: Geophysics, **48,** 665–676.

Debeye H. W., 1995, Seismic character inversion: 65th Annual International Meeting, SEG, Extended Abstracts, 1077–1080.

Francis A., 1997, Acoustic impedance inversion pitfalls and some fuzzy analysis: The Leading Edge, **26**, 275–280.

Huang X., M. Kelkar, A. Chopra, and C. T. Yang, 1995, Wavelet sensitivity study on inversion using heuristic combinatorial algorithms: 65th Annual International Meeting, SEG, Expanded Abstract, 1088–1090.

Levy S., and P. K. Fullagar, 1981, Reconstruction of a sparse spike train from a portion of its spectrum and application to high-resolution deconvolution: Geophysics, **46**, 1235–1243.

Lindseth R.O., 1979, Synthetic sonic logs: a process for stratigraphic interpretation: Geophysics, **44**, 3–26.

Maver K. G., K. B. Rasmussen, J. M. Pedersen, and P. Skjellerup, 1994, Global stochastic seismic inversion with variable prior knowledge for lithology prediction: 64th Annual International Meeting, SEG, Expanded Abstracts, 1024–1027.

Peterson R. A., W. R. Fillipone, and F. B. Coker, 1955, The synthesis of seismograms from well log data: Geophysics, **20**, 516–538.

Sengbush R. L., P. L. Lawrence, and F. J. McDonal, 1961, Interpretation of synthetic seismograms: Geophysics, **26**, 138–157.

Walker C., and T. J. Ulrych, 1983, Autoregressive recovery of the acoustic impedance: Geophysics, **48**, 1338–1350.